

# Spin and interaction effects in quantum dots: a Hartree-Fock-Koopmans approach

Y. Alhassid and S. Malhotra

Center for Theoretical Physics, Sloane Physics Laboratory, Yale University, New Haven, Connecticut 06520, USA

We use a Hartree-Fock-Koopmans approach to study spin and interaction effects in a diffusive or chaotic quantum dot. In particular, we derive the statistics of the spacings between successive Coulomb-blockade peaks. We include fluctuations of the matrix elements of the two-body screened interaction, surface-charge potential, and confining potential to leading order in the inverse Thouless conductance. The calculated peak-spacing distributions are compared with a recent experiment, both in the absence and presence of a magnetic field.

The traditional description of Coulomb blockade in quantum dots has been the constant-interaction (CI) model, where the electrons occupy single-particle levels in a confining potential, and the interaction is taken as a constant charging energy. In dots with chaotic dynamics, the fluctuations of the single-particle levels and wave functions can be described by random-matrix theory (RMT). The CI plus RMT model was successful in describing some of the observed statistical properties of such dots, e.g., the conductance peak-height distribution [1,2]. However, several experiments have demonstrated that other statistics, such as the distribution of the spacing between Coulomb-blockade peaks, are affected by electron-electron interactions [3–6].

At low temperatures the peak spacing is given by the second-order difference of the ground-state energy versus the number of electrons. In the CI model and for spin-degenerate levels, the peak-spacing distribution is bimodal, i.e., a superposition of a  $\delta$  function and a (shifted) Wigner-Dyson distribution. However, none of the measured distributions are bimodal and they all deviate from Wigner-Dyson statistics [3–6].

In the spinless case, Hartree-Fock (HF) calculations [7] and a random interaction matrix model [8] explained the deviation from Wigner-Dyson statistics as an interaction effect. Spin degrees of freedom were included using exact diagonalization for dots with a small number of electrons and small values of the Thouless conductance  $g$  [9]. More recently, spin effects were studied in the limit  $g \rightarrow \infty$  [10–12], using the so-called universal Hamiltonian [13,14]. Interaction effects were studied (in the presence of a magnetic field) using a Strutinsky approach for quantum dots [11]. The resulting distributions showed qualitative differences when compared with the experiments. Temperature effects were shown to be important at temperatures as low as  $T \sim 0.1 - 0.2\Delta$  [12] ( $\Delta$  is the mean spacing between spin-degenerate levels). The spacing statistics were also studied in a spin density functional theory for dots with  $\sim 10$  electrons [15].

Here we develop a theory that includes spin and interaction effects and is based on a HF-Koopmans approach. The theory is generic and does not require the actual solution of the HF equations. Rather than using

the non-interacting basis, we choose as a reference state the  $n$ -electron dot with spin  $S = 0$  ( $n$  even) and work in its HF basis. We then consider the addition energies and the energy differences between various spin configurations in Koopmans' limit where the single-particle wave functions do not change [16]. Previously, Koopmans' approach was discussed for dots with *spinless* electrons [7] and was used to study spectral scrambling [17]. Here we derive the generic statistics of the spin and peak spacings, assuming that the HF levels of the reference state satisfy statistics typical of a diffusive or chaotic dot. The theory is valid for large  $g$ , and for  $g \rightarrow \infty$  it reduces to the universal Hamiltonian [13]. For finite  $g$ , we include fluctuations of the diagonal matrix elements to leading order in  $1/g$ . In contrast to Ref. [11], our theory requires the statistics of only a few levels around the Fermi energy, and some of its results are qualitatively different.

The Hamiltonian of the quantum dot in the “disorder” basis  $|i\sigma\rangle = a_{i\sigma}^\dagger|0\rangle$  ( $\alpha$  denotes a spatial orbit and  $\sigma = \pm 1$  is the spin variable) is given by

$$H = \sum_{i\sigma} \epsilon_i^{(0)} a_{i\sigma}^\dagger a_{i\sigma} + \frac{1}{2} \sum_{\substack{ijkl \\ \sigma\sigma'}} v_{ij;kl} a_{i\sigma}^\dagger a_{j\sigma'}^\dagger a_{l\sigma'} a_{k\sigma}, \quad (1)$$

where  $\epsilon_i^{(0)}$  are the single-particle energies and  $v_{ij;kl}$  are the (spin-independent) matrix elements of the Coulomb interaction. The Hamiltonian (1) can be solved in the HF approximation. For each value of the spin projection  $S_z$ , we use Slater determinants with  $n_+$  ( $n_-$ ) spin up (down) orbitals. Usually, the HF single-particle energies  $\epsilon_{\alpha\sigma}^{(n)}$  and orbitals  $\phi_{\alpha\sigma}$  depend on the spin  $\sigma$ . However for even  $n$ , the HF equations have a solution where  $\epsilon_{\alpha}^{(n)}$  and  $\phi_{\alpha}$  are independent of  $\sigma$ , and the lowest  $n/2$  levels are doubly occupied. Such a Slater determinant has good  $S = 0$ . We choose this solution as our reference state, and work in its HF basis  $|\alpha\rangle$ . This  $S = 0$  state is an eigenstate of the following diagonal many-particle Hamiltonian

$$H_d = \sum_{\alpha\sigma} \epsilon_{\alpha\sigma}^{(0)} \hat{n}_{\alpha\sigma} + \frac{1}{2} \sum_{\substack{\alpha\beta \\ \sigma}} v_{\alpha\beta}^A \hat{n}_{\alpha\sigma} \hat{n}_{\beta\sigma} + \sum_{\alpha\beta} v_{\alpha\beta} \hat{n}_{\alpha+} \hat{n}_{\beta-}, \quad (2)$$

where  $\hat{n}_{\alpha\sigma}$  is the number operator of the state  $\alpha\sigma$ , and

$v_{\alpha\beta} \equiv v_{\alpha\beta;\alpha\beta}$ ,  $v_{\alpha\beta}^{\text{ex}} \equiv v_{\alpha\beta;\beta\alpha}$ , and  $v_{\alpha\beta}^A \equiv v_{\alpha\beta} - v_{\alpha\beta}^{\text{ex}}$  are diagonal, exchange and antisymmetrized matrix elements, respectively.

The Hamiltonian (2) also has eigenstates with  $S \neq 0$ . We label by  $\alpha = 0$  the last occupied level of the  $S = 0$  state. The lowest state for each spin  $S$  is obtained by promoting  $S$  spin down electrons from  $\alpha = 0, \dots, -(S-1)$  to spin up electrons in  $\alpha = 1, \dots, S$ . The resulting Slater determinant describes a maximal spin projection state  $S_z = S$  and has good spin  $S$ . Using (2), the energy difference  $\delta E_n(S) \equiv E_n(S) - E_n(S=0)$  between the lowest states with spin  $S$  and spin  $S=0$  can be written in terms of  $\epsilon_\alpha^{(n)}$  and a few matrix elements. For example

$$\delta E_n(S=1) = (\epsilon_1^{(n)} - \epsilon_0^{(n)}) - v_{10}. \quad (3)$$

The spin  $S_n$  of the ground state of the  $n$ -electron dot is determined by minimizing  $\delta E_n(S)$ .

Similarly, the ground-state spin  $S_{n+1}$  of the dot with  $n+1$  electrons can be determined from the energy differences  $\delta E_{n+1}(S) \equiv E_{n+1}(S) - E_{n+1}(S=1/2)$  for half-integer  $S$ . Assuming Koopmans' limit, we can express  $\delta E_{n+1}(S)$  in terms of the HF levels and matrix elements of the reference state ( $n, S=0$ ). For example

$$\delta E_{n+1}(S=3/2) = (\epsilon_2^{(n)} - \epsilon_0^{(n)}) - v_{10} - v_{20} + v_{21}^A. \quad (4)$$

The addition energy  $\mu_{n+1} \equiv E_{\text{gs}}(n+1) - E_{\text{gs}}(n)$  is

$$\mu_{n+1} = \mu_{n+1}(0 \rightarrow 1/2) + \delta E_{n+1}(S_{n+1}) - \delta E_n(S_n), \quad (5)$$

where in Koopmans' limit  $\mu_{n+1}(0 \rightarrow 1/2) = \epsilon_1^{(n)}$ .

The spacing  $\Delta_2$  between successive peaks is given by the difference in addition energies. We have to distinguish between even-odd-even ("odd") and odd-even-odd ("even") transitions (in particle number). We consider here the odd transition  $n \rightarrow n+1 \rightarrow n+2$  ( $n$  even), for which  $\Delta_2 = \mu_{n+2} - \mu_{n+1}$  (similar results can be derived for the even transition [18]).  $\mu_{n+1}$  is given by (5) and  $\mu_{n+2}$  is calculated from  $\mu_{n+2} = \mu_{n+2}(1/2 \rightarrow 0) + \delta E_{n+2}(S_{n+2}) - \delta E_{n+1}(S_{n+1})$  with  $\mu_{n+2}(1/2 \rightarrow 0) = \epsilon_1^{(n)} + v_{11}$ .  $\delta E_{n+1}(S)$  is given by, e.g., Eq. (4), while  $\delta E_{n+2}(S)$  is calculated from, e.g.,

$$\delta E_{n+2}(S=1) = (\epsilon_2^{(n)} - \epsilon_1^{(n)}) - v_{11} + v_{21}^A. \quad (6)$$

To describe the statistics of  $\Delta_2$  it is necessary to model the fluctuations of the HF levels and wave functions of the ( $n, S=0$ ) dot. The spectrum is assumed to follow RMT within  $g$  levels around the Fermi energy, and the matrix elements are uncorrelated from the single-particle spectrum. An exception is the gap  $\epsilon_1^{(n)} - \epsilon_0^{(n)}$ . We find its statistics by comparing the single-particle spectrum of the ( $n+2$ )-electron dot with the spectrum of the  $n$ -electron dot (both in their  $S=0$  configuration). We have the relation  $\epsilon_1^{(n)} - \epsilon_0^{(n)} = \epsilon_1^{(n+2)} - \epsilon_0^{(n+2)} + v_{01}^A + v_{01} - v_{11}$ , in

which the levels  $\epsilon_0^{(n+2)}$  and  $\epsilon_1^{(n+2)}$  are both doubly occupied, and thus their spacing should follow Wigner-Dyson statistics. The gap distribution is then a convolution of a Wigner-Dyson distribution with a Gaussian describing the distribution of  $v_{01}^A + v_{01} - v_{11}$  (see below).

We decompose the interaction in (2) into its average and fluctuating parts, and denote by  $U_d = \bar{v}_{\alpha\beta}$  and  $J_s = \bar{v}_{\alpha\beta}^{\text{ex}}$  ( $\alpha \neq \beta$ ) the average values of the direct and exchange interaction, respectively. The average interaction is invariant under a change of the single-particle basis when  $\bar{v}_{\alpha\alpha} = U_d + J_s$  and can be written in terms of the number operator  $\hat{n}$  and total spin  $\mathbf{S}$  [19]

$$\bar{V} = (U_d - J_s/2)\hat{n}(\hat{n}+2)/2 - J_s\mathbf{S}^2. \quad (7)$$

To estimate  $U_d$  and  $J_s$ , we replace the long-range bare Coulomb interaction by an effective interaction. In the limit  $r_s \ll 1$ , an effective RPA interaction is  $v(\mathbf{r}_1, \mathbf{r}_2) = e^2/C + v_\kappa(\mathbf{r}_1, \mathbf{r}_2) + V(\mathbf{r}_1) + V(\mathbf{r}_2)$ , where  $v_\kappa(\mathbf{r}_1, \mathbf{r}_2)$  is the bulk two-body screened interaction, and  $V(\mathbf{r})$  is a one-body potential generated by the accumulation of surface charge in the finite geometry of the dot [20].

The average interaction is determined by the spatial correlations of the single-particle wave functions [20,21]. To leading order in  $1/g$ ,  $U_d - e^2/C = J_s = (\Delta/2)(1 + 2\beta^{-1}b_1/g)$  [22]. The geometry-dependent coefficient  $b_1$  is determined from  $b_1/g = \int d\mathbf{r}\Pi(\mathbf{r}, \mathbf{r})/\mathcal{A}$ , where  $\Pi(\mathbf{r}_1, \mathbf{r}_2)$  is the diffuson propagator and  $\mathcal{A}$  is the area of the dot.

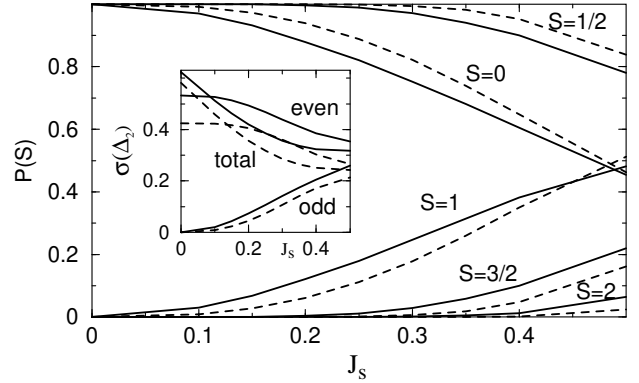


FIG. 1. Statistics in the absence of fluctuations of the interaction matrix elements. The probabilities of various spin values  $S$  are shown versus  $J_s$ . The solid (dashed) lines describe the orthogonal (unitary) symmetry. Inset: the standard deviation of the peak spacing  $\sigma(\Delta_2)$  versus  $J_s$  for the even, odd and combined ("total") transitions.  $J_s$  and  $\sigma(\Delta_2)$  are measured in units of  $\Delta$ .

Koopmans' limit is exact when the fluctuations of the matrix elements are ignored, and our calculations of  $\Delta_2$  reduce to those in Ref. [10], i.e., they can be derived directly from an Hamiltonian that consists of a random one-body part plus an average interaction (7). In the limit  $g \rightarrow \infty$  this Hamiltonian is just the universal Hamiltonian with  $J_s = \Delta/2$  [13,14]. A better estimate of  $J_s$

can be obtained in RPA [10]; it increases monotonically with  $r_s$  but remains below  $\Delta/2$ .

In the simple limit (7), the spin and spacing distributions are determined by a single parameter  $J_s/\Delta$  [10]. This limit is demonstrated in Fig. 1 where we show the probabilities of various spin values versus  $J_s$ . The inset shows the standard deviation of  $\Delta_2$  versus  $J_s$  for the even and odd transitions as well as the combined one (“total”).

Next we discuss the fluctuations of the interaction matrix elements, which are approximately Gaussian variables. We discuss separately the bulk screened interaction and surface-charge potential. Using the diagrammatic approach for the two-body screened interaction, we have, for  $r_s \ll 1$  and to leading order in  $1/g$

$$\begin{aligned} \text{GOE} : \sigma(v_{\alpha\beta}) &= 2\sigma_2; \quad \sigma(v_{\alpha\beta}^{\text{ex}}) = \sqrt{2}\sigma_2; \quad \sigma(v_{\alpha\alpha}) = 2\sqrt{2}\sigma_2 \\ \text{GUE} : \sigma(v_{\alpha\beta}) &= \sigma_2; \quad \sigma(v_{\alpha\beta}^{\text{ex}}) = \sigma_2; \quad \sigma(v_{\alpha\alpha}) = \sqrt{2}\sigma_2. \end{aligned} \quad (8)$$

Different matrix elements (including the direct  $v_{\alpha\beta}$  and exchange  $v_{\alpha\beta}^{\text{ex}}$ ) are uncorrelated. We note that the values in (8) are different from those obtained for a zero-range interaction [23]. The parameter  $\sigma_2$  is given by

$$\sigma_2 = \left[ \mathcal{A}^{-2} \int d\mathbf{r}_1 \int d\mathbf{r}_2 \Pi^2(\mathbf{r}_1, \mathbf{r}_2) \right]^{1/2} = c_2 \Delta/g, \quad (9)$$

where  $c_2$  is a geometry-dependent coefficient. For a disk of radius  $R$  and boundary conditions of vanishing normal derivative, we find [18]  $c_2 = 2[\sum_{l,m} x_{l,m}^{-4}]^{1/2} \approx 0.94$  where  $x_{l,m}$  are the zeros of  $J_l'(x)$  ( $J_l$  is the Bessel function of order  $l$ ) and  $g\Delta = 2\pi\hbar D/R^2$  ( $D$  being the diffusion constant). Since only a few matrix elements contribute to the peak spacing, the contribution of the two-body screened interaction is parametrically of the order  $\Delta/g$ , unlike the  $\Delta/\sqrt{g}$  dependence found in Ref. [11].

The surface-charge contribution to an interaction matrix element is  $v_{\alpha\beta} = V_\alpha + V_\beta$ , where  $V_\alpha = \int |\psi_\alpha(\mathbf{r})|^2 V(\mathbf{r})$  is a diagonal matrix element of the surface-charge potential. We have

$$\sigma(V_\alpha) = (2/\beta)^{-1/2} \sigma_1; \quad \overline{V_\alpha V_\beta} - \overline{V_\alpha} \overline{V_\beta} \approx 0, \quad (10)$$

where

$$\begin{aligned} \sigma_1 &= \left[ 2\mathcal{A}^{-2} \int d\mathbf{r}_1 \int d\mathbf{r}_2 V(\mathbf{r}_1) \Pi(\mathbf{r}_1, \mathbf{r}_2) V(\mathbf{r}_2) \right]^{1/2} \\ &= c_1 \Delta/\sqrt{g}. \end{aligned} \quad (11)$$

For a 2D circular disk of radius  $R$  and a large distant gate, the surface-charge potential can be approximated by  $V(\mathbf{r}) = -(e^2/2\kappa R)(R^2 - r^2)^{-1/2}$ , where  $\kappa = 2\pi e^2\nu/\epsilon$  is the inverse screening length ( $\epsilon$  is the dielectric constant) [20]. We then find  $c_1 = 2^{-1/2}[\sum_{m \neq 0} \sin^2 x_{0,m}/(x_{0,m}^4 J_0^2(x_{0,m}))]^{1/2} \approx 0.087$  [18].

The above results can be generalized to a ballistic dot, using the ballistic supersymmetric  $\sigma$  model obtained

when a weak disorder with finite correlation length is added [24]. In particular, if the disorder Lyapunov length is smaller than the dot’s size, results similar to Eqs. (8) can be derived but with the ballistic propagator  $\Pi_B$  replacing the diffusive  $\Pi$ . The ballistic Thouless conductance of, e.g., a circular dot with  $n$  electrons is obtained from the inverse time it takes to cross the diameter  $2R$  of the dot, leading to  $g = \pi k_F R/2 = \pi(n/2)^{1/2}$ . In the ballistic case  $\sigma_2$  contains a logarithmic factor, i.e.,  $\sigma_2 = c_2 \Delta[\ln(c_2'g)]^{1/2}/g$ . The direct propagation between  $\mathbf{r}_1$  and  $\mathbf{r}_2$  contributes to  $\Pi_B(\mathbf{r}_1, \mathbf{r}_2)$  a term  $1/(\pi k_f |\mathbf{r}_1 - \mathbf{r}_2|)$  which is just the smooth part of  $J_0^2(k_F |\mathbf{r}_1 - \mathbf{r}_2|)$ . The remaining part involves single or multiple scattering from the boundaries and requires knowledge of the semiclassical dynamics. It can be calculated analytically for a circular billiard with diffusive boundaries [25]. Using this model, we estimate  $c_2 = 0.85$  and  $c_2' = 2.33$  [18]. A similar estimate of (11) gives  $c_1 = 0.44$ .

We have studied the effects of fluctuations of the interaction matrix elements on the peak-spacing distribution. In Fig. 2 we show the standard deviation  $\sigma(\Delta_2)$  versus  $\sigma_1$  ( $J_s = 0.3\Delta$  and  $\sigma_2 = 0.05\Delta$ ) for the orthogonal (solid lines) and unitary (dashed lines) symmetries.  $\sigma(\Delta_2)$  increases with  $\sigma_1$  and it does so faster in the odd case.

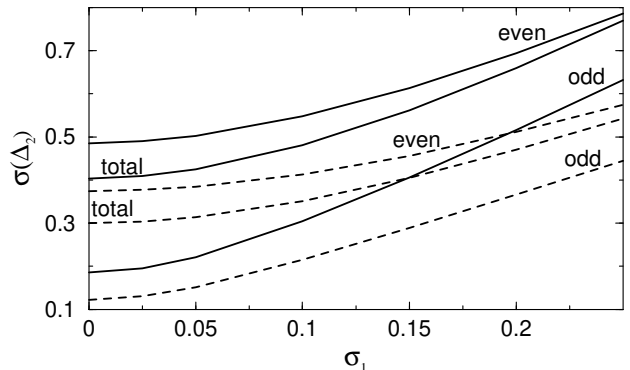


FIG. 2. The standard deviation  $\sigma(\Delta_2)$  versus the standard deviation  $\sigma_1$  of the surface-charge potential for  $J_s = 0.3\Delta$  and  $\sigma_2 = 0.05\Delta$ . The solid and dashed lines describe the orthogonal and unitary symmetries, respectively.

Fig. 3 shows typical peak-spacing distributions for both the orthogonal (left) and unitary (right) symmetries for  $\sigma_2 = 0.025\Delta$  and  $\sigma_1 = 0, 0.05\Delta$  and  $0.1\Delta$ . Signatures of the bimodality can still be observed for  $\sigma_1 = 0$  but they disappear at  $\sigma_1 = 0.05\Delta$ . Nevertheless, the distributions remain asymmetric (more so in the unitary case).

An additional contribution to the fluctuations of  $\Delta_2$  arises from the variation of the gate voltage between peaks. In general, the change of the gate voltage between two peaks leads to a spatially non-uniform change  $U(\mathbf{r}) = -V(\mathbf{r}) + \tilde{V}(\mathbf{r})$  in the confining potential, where  $\tilde{V}$  originates in the mutual dot-gate capacitance [14]. This leads to scrambling of the HF levels between peaks. For example, let us consider the odd transition. As the gate

voltage changes between  $V_g^{n+1}$  and  $V_g^{n+2}$ , the reference HF levels  $\epsilon_\alpha^{(n)}$  change by  $\delta\epsilon_\alpha^{(n)} \approx U_\alpha = \int d\mathbf{r} |\psi_\alpha(\mathbf{r})|^2 U(\mathbf{r})$ . We therefore substitute  $\epsilon_\alpha \rightarrow \epsilon_\alpha + U_\alpha$  in the calculation of  $\mu_{n+2}$  and in Eq. (6) ( $\mu_{n+1}$  is unchanged and calculated from Eq. (5)). This level scrambling can also lead to spin rearrangement in the dot. The ground-state spin of the  $n+1$ -electron dot at gate voltage  $V_g^{n+2}$  (just below the transition) is found from (6) (and its generalization to higher values of  $S$ ) after the substitution  $\epsilon_\alpha \rightarrow \epsilon_\alpha + U_\alpha$ .

The fluctuations properties of  $U_\alpha$  are similar to those of  $V_\alpha$  in Eqs. (10), except that  $V(\mathbf{r})$  is replaced by  $U(\mathbf{r})$  in Eq. (11). For a large distant gate, we expect the potential on the dot to change uniformly and there is no scrambling due to the gate voltage.

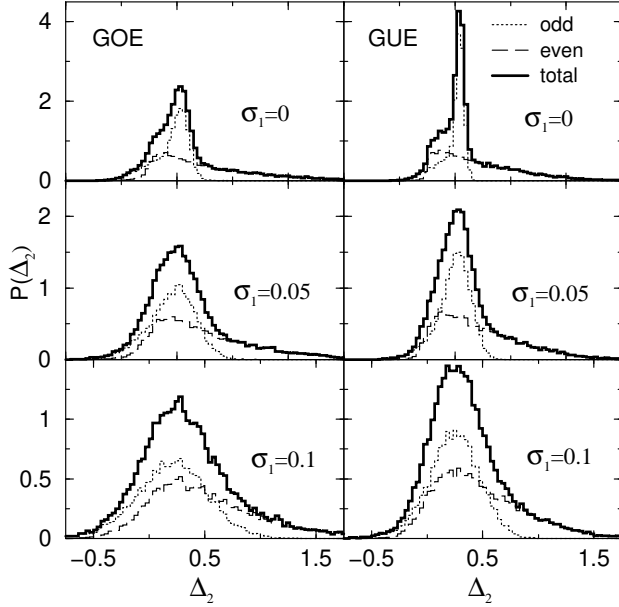


FIG. 3. Peak-spacing distributions  $P(\Delta_2)$  for the orthogonal (left) and unitary (right) symmetries and for  $\sigma_1 = 0, 0.05\Delta$  and  $0.1\Delta$ . In all cases  $J_s = 0.3\Delta$  and  $\sigma_2 = 0.025\Delta$ . The bimodality is lost already for  $\sigma_1 = 0.05\Delta$  but the distributions remain asymmetric.

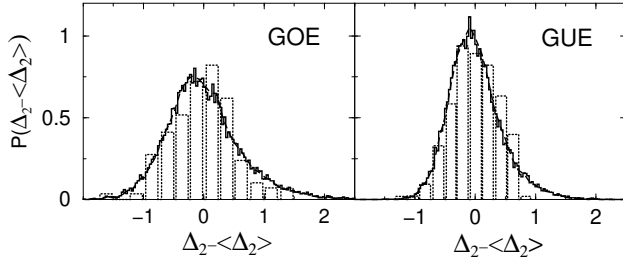


FIG. 4. Calculated peak-spacing distributions (solid lines) with  $J_s = 0.3\Delta$ ,  $\sigma_1 = 0.18\Delta$  and  $\sigma_2 = 0.063\Delta$  are compared with the experimental results of Ref. [6] (dotted histograms) for both the orthogonal (left) and unitary (right) symmetries. The dashed lines are the finite temperature distributions ( $T = 0.05\Delta$ ) and are almost indistinguishable from the solid lines.

We now consider whether the experimental distributions of Ref. [6] can be described by our theory. Special effort was taken in the experiment to minimize deformation effects, and we ignore gate voltage scrambling. It is difficult to estimate  $\sigma_1$  and  $\sigma_2$  for the ballistic dot used in the experiment. The simple estimates based on a billiard with surface scattering (see the second paragraph after Eq. (11)) for  $n \approx 190$  electrons (i.e.,  $g \approx 30.6$ ) give  $\sigma_1 = 0.08\Delta$  and  $\sigma_2 = 0.059\Delta$ . We have fixed  $\sigma_2$  at its estimated value and found that a reasonable description of the experimental data [6] can be obtained for  $\sigma_1 \approx 0.18\Delta$ . Fig. 4 compares the theoretical distributions (solid histograms) with the experiment (dotted histograms). The agreement is reasonable for both the orthogonal and unitary symmetries even though the same parameters are used for both cases. The temperature in the experiment  $T \approx 0.05\Delta$  is low, and its inclusion affects only slightly the calculated distributions (dashed lines) [18].

In conclusion, we have developed a HF-Koopmans approach to study spin and interaction effects in diffusive or chaotic quantum dots. In particular we have studied the dependence of the peak-spacing distribution on the fluctuations of the interaction matrix elements to leading order in the inverse Thouless conductance.

This work was supported in part by the U.S. DOE grant No. DE-FG-0291-ER-40608. We acknowledge useful discussions with Y. Gefen and A. Polkovnikov, and in particular with A.D. Mirlin.

- 
- [1] Y. Alhassid, Rev. Mod. Phys. **72**, 895 (2000).
  - [2] R.A. Jalabert, A.D. Stone, and Y. Alhassid, Phys. Rev. Lett. **68**, 3468 (1992).
  - [3] U. Sivan *et al.*, Phys. Rev. Lett. **77**, 1123 (1996).
  - [4] F. Simmel, T. Heinzel and D.A. Wharam, Europhys. Lett. **38**, 123 (1997).
  - [5] S.R. Patel *et al.*, Phys. Rev. Lett. **80**, 4522 (1998).
  - [6] S. Lüscher *et al.*, Phys. Rev. Lett. **86**, 2114 (2001).
  - [7] S. Levit and D. Orgad, Phys. Rev. B **60**, 5549 (1999); P.N. Walker, G. Montambaux, and Y. Gefen, Phys. Rev. B **60**, 2541 (1999); A. Cohen, K. Richter, and R. Berkovits, Phys. Rev. B **60**, 2536 (1999).
  - [8] Y. Alhassid, Ph. Jacquod, and A. Wobst, Phys. Rev. B **61**, R 13357 (2000).
  - [9] R. Berkovits, Phys. Rev. Lett. **81**, 2128 (1998).
  - [10] Y. Oreg, P.W. Brouwer, X. Waintal, and B.I. Halperin, cond-mat/0109541 (2001).
  - [11] D. Ullmo and H.U. Baranger, Phys. Rev. B **64**, 245324 (2001).
  - [12] G. Usaj and H.U. Baranger, Phys. Rev. B **64**, 201319(R) (2001).
  - [13] I.L. Kurland, I.L. Aleiner, and B.L. Altshuler, Phys. Rev. B **62**, 14886 (2000).
  - [14] I.L. Aleiner, P.W. Brouwer, and L.I. Glazman, Phys.

Rep. **358**, 309 (2002).

- [15] K. Hirose and N.S. Wingreen, cond-mat/0202266.
- [16] T. Koopmans, Physica (Amsterdam) **1**, 104 (1934).
- [17] Y. Alhassid and Y. Gefen, cond-mat/0101461.
- [18] Y. Alhassid and S. Malhotra, to be published.
- [19] More generally, an additional Cooper channel interaction  $J_c = \bar{v}_{\alpha\alpha;\beta\beta}$  can contribute to (7) in the orthogonal case.
- [20] Ya. M. Blanter, A.D. Mirlin, and B.A. Muzykantskii, Phys. Rev. Lett. **78**, 2449 (1997).
- [21] A.D. Mirlin, Phys. Rep. **326**, 260 (2000).
- [22] Here we approximate the screened interaction by a contact interaction  $(\Delta/2)\mathcal{A}\delta(\mathbf{r}_1 - \mathbf{r}_2)$ .
- [23] A.D. Mirlin, private communication.
- [24] I.V. Gornyi and A.D. Mirlin, cond-mat/0107552.
- [25] Ya. M. Blanter, A.D. Mirlin, and B.A. Muzykantskii, Phys. Rev. B **63** 235315 (2001).